

## Thermographic study of the pathological manifestations due to humidity and of the conservation state of the Santa Maria Basilica's roof

D. Bru<sup>1</sup>\*, S. Ivorra<sup>1</sup>\*Contact author: [david.bru@ua.es](mailto:david.bru@ua.es)DOI: <https://doi.org/10.21041/ra.v12i1.567>

Reception: 01/11/2021 | Acceptance: 13/12/2021 | Publication: 01/01/2022

### ABSTRACT

This paper analyzes the current state of the roof of the Basilica of Santa Maria, Alicante, Spain. This building dates back to the 13th century and is catalogued. For the analysis of the efflorescence observed, an analysis of the constructive typology is carried out, as well as a visual analysis of the state of the same, describing the existing pathological manifestations, both in the exterior area of the roofs, as well as in the interior area of the rooms under them. For the technical analysis of the possible leaks from the roof to the interior rooms of the basilica, a watertightness test and the verification through the control of the variation of temperatures by means of thermographic analysis are carried out. It can be concluded the existence and position of leaks that have damaged this listed building.

**Keywords:** thermography, humidities, filtrations, efflorescence, historical building.

**Cite as:** Bru, D., Ivorra, S. (2022), “*Thermographic study of the pathological manifestations due to humidity and of the conservation state of the Santa Maria Basilica's roof*”, Revista ALCONPAT, 12 (1), pp. 110 – 126, DOI: <https://doi.org/10.21041/ra.v12i1.567>

<sup>1</sup>Departamento de Ingeniería Civil, Escuela Politécnica Superior, Universidad de Alicante, Alicante, España.

#### Contribution of each author

In this work the author David Bru contributed 100% with the data collection and experimentation activity, with the original idea activity, writing of the work and discussion of the results in 50%. The author Salvador Ivorra contributed with the activity of original idea, writing of the work and discussion of the results by 50%.

#### Creative Commons License

Copyright 2022 by the authors. This work is an Open-Access article published under the terms and conditions of an International Creative Commons Attribution 4.0 International License ([CC BY 4.0](https://creativecommons.org/licenses/by/4.0/)).

#### Discussions and subsequent corrections to the publication

Any dispute, including the replies of the authors, will be published in the third issue of 2022 provided that the information is received before the closing of the second issue of 2022.

## **Estudo termográfico das manifestações patológicas devidas à umidade e do estado de conservação da cobertura da Basílica de Santa Maria**

### **RESUMO**

Este trabalho analisa o estado atual da cobertura da Basílica de Santa María, Alicante, Espanha. Este edifício data do século XIII e está catalogado. Para a análise das eflorescências observadas foi efetuada uma análise da tipologia da construção, bem como uma análise visual do estado dela, descrevendo as manifestações patológicas existentes, tanto na zona exterior das coberturas, como na área interna dos ambientes abaixo dela. Para a análise técnica de possíveis vazamentos através da cobertura para os ambientes interiores da basílica, foi efetuado um ensaio de estanqueidade e verificação através do controle da variação de temperatura por meio de análise termográfica. O procedimento foi adequado para entender e comprovar a existência e localização de vazamentos que danificaram este edifício.

**Palavras-chave:** termografia, umidade, infiltração, eflorescência, edifício histórico.

## **Estudio termográfico de las manifestaciones patológicas por humedades y del estado de conservación de la cubierta de la Basílica de Santa María**

### **RESUMEN**

El presente trabajo analiza el estado actual de la cubierta de la Basílica de Santa María, Alicante, España. Este edificio data del siglo XIII y está catalogado. Para el análisis de las eflorescencias que se observan se realiza un análisis de la tipología constructiva, así como un análisis visual del estado de las mismas, describiendo las manifestaciones patológicas existentes, tanto en la zona exterior de las cubiertas, como en la zona interior de las salas bajo las mismas. Para el análisis técnico de las posibles filtraciones de la cubierta a las salas interiores de la basílica se realiza una prueba de estanquidad y la verificación a través del control de la variación de temperaturas mediante análisis termográfico. Se puede concluir la existencia y posición de filtraciones que han dañado este edificio catalogado.

**Palabras clave:** termografía, humedades, filtraciones, eflorescencias, edificio histórico.

### **Legal Information**

Revista ALCONPAT is a quarterly publication by the Asociación Latinoamericana de Control de Calidad, Patología y Recuperación de la Construcción, Internacional, A.C., Km. 6 antigua carretera a Progreso, Mérida, Yucatán, 97310, Tel.5219997385893, [alconpat.int@gmail.com](mailto:alconpat.int@gmail.com), Website: [www.alconpat.org](http://www.alconpat.org)

Reservation of rights for exclusive use No.04-2013-011717330300-203, and ISSN 2007-6835, both granted by the Instituto Nacional de Derecho de Autor. Responsible editor: Pedro Castro Borges, Ph.D. Responsible for the last update of this issue, Informatics Unit ALCONPAT, Elizabeth Sabido Maldonado.

The views of the authors do not necessarily reflect the position of the editor.

The total or partial reproduction of the contents and images of the publication is carried out in accordance with the COPE code and the CC BY 4.0 license of the Revista ALCONPAT.

## 1. INTRODUCTION

The purpose of this work is the technical assessment of the current pathological manifestations of the waterproofing system in the roof of the Basilica of Santa Maria, Alicante, Spain, Figure 1. The Basilica of Santa Maria, located at coordinates 38°20'46"N 0°28'45"W and less than 300 m from the coastline, has been catalogued as an Asset of Cultural Interest within the monuments listed in the Valencian Cultural Heritage. The oldest parts of the building have been dated between the 13th and 14th centuries. From the architectural point of view, the structure has a single nave without transept, with side chapels located between the buttresses and a polygonal apse, Figure 2. The main nave is covered by six ribbed vaults with pointed arches, separated from each other by toral arches, which together with the ribs start from the capital in a solution typical of the late fifteenth century and the first decades of the sixteenth century (Beviá et al, 1997).

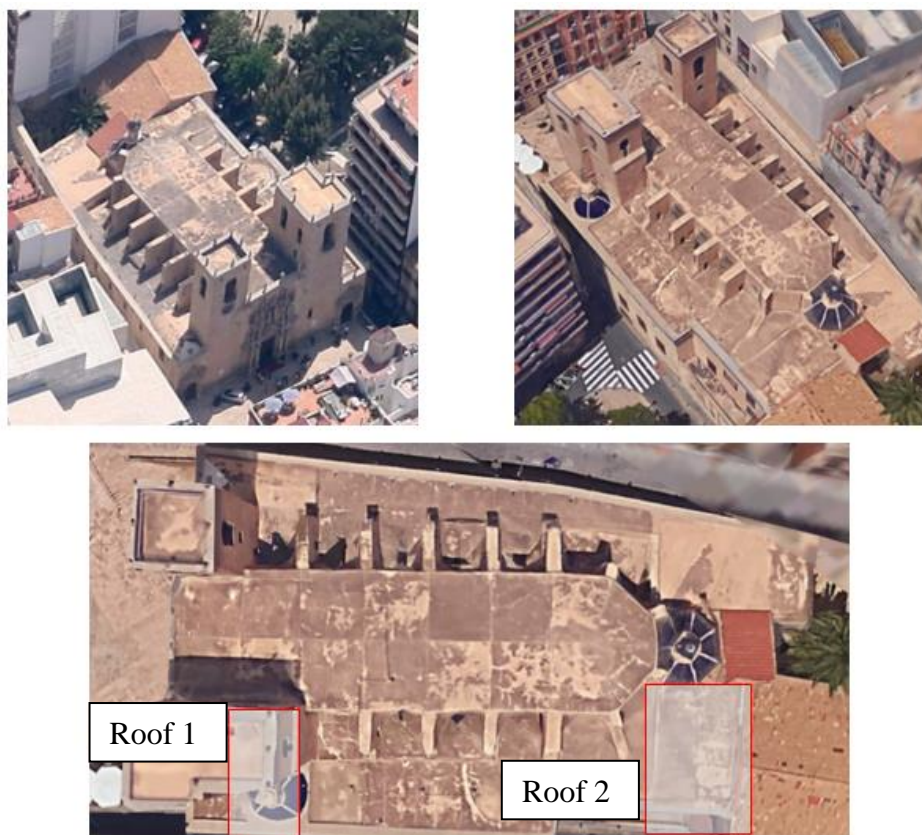


Figure 1. Aerial view of the Basilica of Santa María, Alicante. Sup. left: northwest facade. Sup. right: Southeast facade. Below: Plan view of the Basilica of Santa Maria, Alicante. Identification of study roofs. Source: Images ©2016 Google, Map data ©2016 Google, Inst. Geogr. Nacional.

Regarding the main materials that constitute the masonry elements of the Basilica of Santa Maria, no laboratory studies have been carried out to identify their origin. However, and according to the historical data, we provide in the present investigation the data associated with the rocks of the same origin arranged in the Civil Palaces of Gravina Street (Louis et al. 2001), close to the location of the Basilica. The data obtained from this research allow us to classify the typology of the rock used, its compressive strength and absorption coefficient. In this sense, the rock consists of a biocalcarene with variable grain size, from medium to coarse sand and even microconglomerate (>2mm), with a high porosity and a compressive strength of 6.1 MPa. On the other hand, in relation to the absorption coefficient, values between 6% and 15% are shown. In this sense, it is important

to highlight the high value of the same in comparison with other limestone or marl type stones, with values between 0.56% and 2.05% (Thomas et al. 2008). Other data associated with the calcite content and density of this material are shown in Table 1.

Finally, Louis et al (2001), also highlight an important aspect for the analysis of pathologies due to the presence of moisture in this type of materials. Specifically, they evaluate the presence of efflorescence and highlight the highly detrimental effect of salt crystallization in the process of alveolar erosion and especially in areas with facades exposed to the sea wind, since this effect favors the crystallization of salts and contributes with a large amount of sea salt due to the sea spray effect. These statements are confirmed by the presence of halite in the efflorescence on the inside of the structure. In addition, they show that part of the sodium chloride from the marine environment or from the infiltration water has reached part of the analyzed building due to capillarity phenomena. Therefore, based on the previous results of Louis et al (2001), the hypothesis of the presence of salts in the constituent materials of the Basilica analyzed can be affirmed.

Table 1. Compositional data and some physical properties of the San Julián Stone (Brotóns et al. 2013).

<b>San Julián Stone</b>	<b>Quarry</b>	<b>Buildings</b>
Calcite (%)	80-85	65-85
Water absorption (%)	7.6-15.1	6.2-13.0
Real density (g/cm <sup>3</sup> )	2.64-2.67	2.59
Apparent density (g/cm <sup>3</sup> )	1.85-2.29	1.8-2.4

The building analyzed in this study is framed within the typologies of historical constructions, being its constructive approach very different from the buildings of today. From the hygrothermal point of view, its main difference is its conception as a building permeable to water (in vapor or liquid form), both from the exterior and from the interior (Paricio, 1985), unlike current buildings that are designed as isolated elements, to avoid the loss of energy to the exterior. Schematically, the building studied, as mentioned in section 1, has a perimeter enclosure that is estimated (with the available means) to have a very thick sheet. This fact causes that, facing the action of external water, the external part of the leaf in contact with the water gets wet and diffuses the water in liquid form through the thickness of the wall. The advance of the water through the wall forms a "wet front" until the precipitation ceases. This amount of water remains absorbed in the masonry due to the high absorption capacity of the constituent materials of the masonry and then evaporates on both sides of the wall. Therefore, it is possible to intuit the importance of the thickness and permeability of the material, in order to prevent the wet front from appearing inside the room and, above all, so that once the source of humidity is finished, the water evaporates in the shortest possible time, especially to avoid overlapping of wet fronts between different precipitation cycles. Therefore, it is also clear that the evacuation of water in this type of building occurs in a deferred manner by diffusion and evaporation. Therefore, it is common to observe in this type of building processes of saturation of the facing by rainwater, once the pores are saturated, and surface runoff processes along the facing, producing the wetting of other areas of the element arranged for the enclosure of the construction.

On the other hand, in relation to the dynamic phenomena of water inside the building in the form of vapor, it is important to note that, due to the absence of plastic sheets or vapor barriers such as those currently used in modern roofs and enclosures, the building was characterized as eminently permeable. It is common for the minimum specific humidity of a room to be the same as that of the outside, since the air is able to penetrate from the outside without being subjected to any barrier process. Therefore, the usual problems of this type of construction when faced with humidity in its

original conception was to try to eliminate the excess vapor generated inside the rooms due to human respiration and perspiration, in order to equalize the specific humidity inside the room to that of the outside. Thus, as mentioned above, if the room did not have windows or openings to eliminate the excess water vapor accumulated in the room, it was eliminated either by diffusion through the walls, convection through openings and slits, or by absorption of the vapor in the materials, which was then transferred to the environment when it was dried.

Once the technical conception of the approach to the enclosure systems of the historic buildings has been considered, it is necessary to analyze the possible causes that generate the formation of damp, since this is the main reason for the writing of this study. The presence of humidity can be due to filtration processes by direct contact with water or by capillarity. In both cases, the transfer of water through the masonry may entail the entrainment of soluble salts, either from the rock itself or from the seepage water itself. Such soluble salts can be retained in the enclosures when the water evaporates, crystallizing in the pores and causing the appearance of efflorescence (Giovannacci et al, 2017). The saturation of the pores due to the presence of salt crystallization decreases the evaporation processes and causes a displacement of the moisture stains due to the search for new exit zones of the water vapor present in the porous materials.

On the other hand, if the accumulation of salts mentioned above corresponded to hygroscopic salts, these would tend to retain water from the air when the relative humidity exceeds a certain limit value, which could generate a false mechanism of the presence of moisture due to hygroscopic condensation, with the possible appearance of stains, but caused simply by the absorption of water vapor from the air due to the effect of the hygroscopicity of the salts and not by the real presence of a source of water by filtration or capillarity. For this reason, a general cause of moisture pathology in historic buildings is the appearance of efflorescence due to local seepage phenomena caused years ago that have subsequently been reactivated. That is to say, the appearance of new moistures on the masonry would not be due to the real presence of a new water seepage, but due to the hygroscopicity of the salts on the surface of the rocks. Grossi and Esbert (Grossi and Esbert, 1994) show a deep bibliographical review on the effects of soluble salts in the deterioration of monumental rocks. In this sense, in the interior of the analyzed church, different efflorescences and stains are observed, which suggest the existence of filtrations, Figure 2.

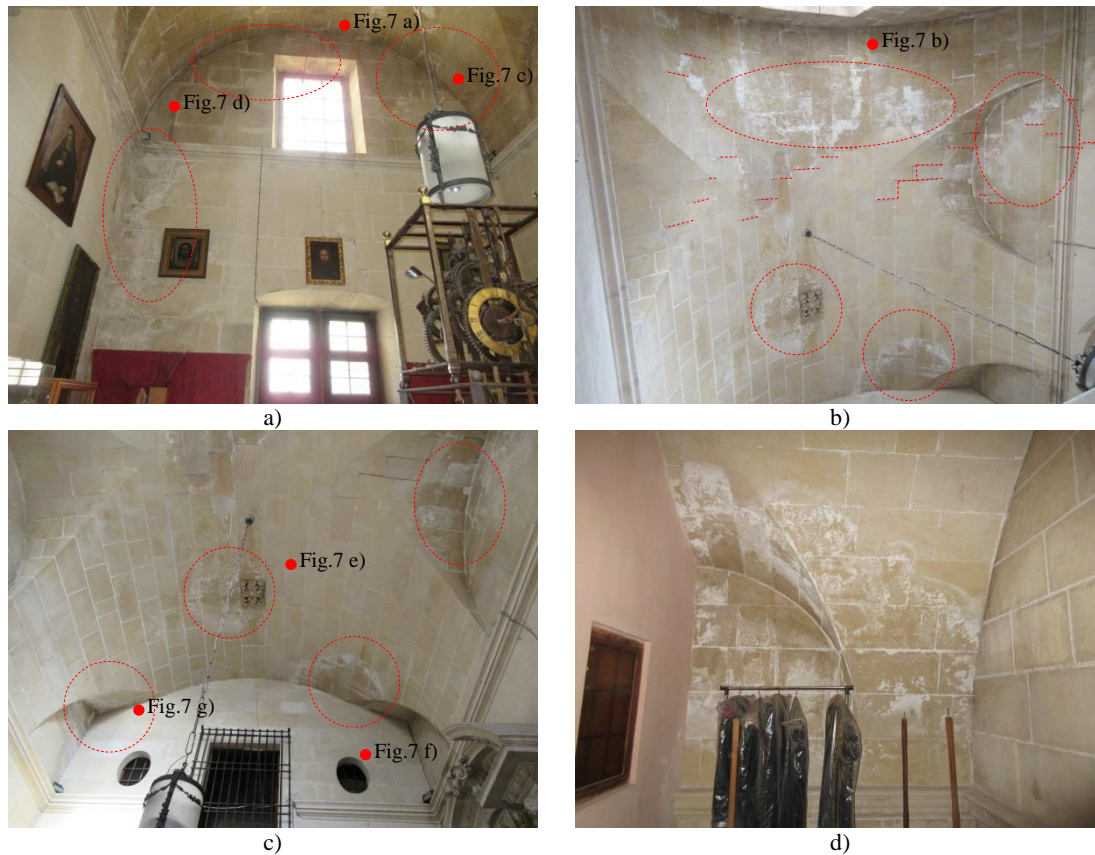


Figure 2. Photos of rooms under roof 2: a) East facade, b) Lower view of the roof, c) Lower view of the roof with vault partition wall, d) Upper adjoining room after division with partition wall. Photos of rooms under roof 1: e) Lower view of the roof area next to the exterior facade, f) Lower view of the roof in contact with the body of the church. Figures a), b), c) include the tomography points of Figure 7 with a red dot.

## 2. EXPERIMENTAL PROGRAM

A comparative visual analysis has been carried out, based on the performance of a watertightness test, analyzing the state of the rooms before and after the flooding process of the roofs, with the aim of detecting leaks with quick access from the roof. Finally, an analysis was performed from infrared thermography of both the roof and the aforementioned rooms, in order to detect the existence of localized thermal bridges and areas of significant moisture presence (Takeda, 2018), (Silva et al, 2019).

In order to determine the general operating conditions of the roof in relation to the slopes, the state of the waterproofing support, as well as the state of execution of the singular elements, such as edges, junctions, drains and joints, it was proposed to perform a watertightness test in order to observe the appearance or not of humidities under the roof or in the walls, paying attention to the critical points associated with construction details according to the regulations in use at the date of waterproofing of the roof (NBE QB-90). The watertightness test consisted of flooding to a level approximately 3-7 cm above the drainage level, ensuring a sufficiently low overload level so as not to affect the structural safety conditions of the roof. The flooding was maintained for 72h, the drains being sealed with a plastic waterproofing system in order to prevent the water level on the roof from decreasing. Finally, once the time required for the watertightness test had elapsed, the sealing systems of the drains were removed in order to maintain their current operation.

On the other hand, in order to determine the presence of humidities and possible thermal bridges, which show an incorrect functioning of the roof, a test was carried out using a FLIR E30 model thermographic camera, based on the provisions of the EN 13187:1998 standard. Some recently published examples of the application of this technique can be found in the following references (Vijay et al, 2019), (Valluzzi et al, 2019), (Lucchi, 2018), (Ruiz Valero, et al, 2019), (Garrido et al, 2020), (Martínez-Garrido et al, 2018), (Zhang et al, 2018), (Barreira et al, 2020) and (Barbosa et al, 2021)).

The test was performed during two consecutive days. During the first day, the thermal recording of decks 1 and 2, as well as the room under room 2, was performed. This recording was carried out between 19:45 and 20:45. The maximum and minimum values ranged throughout the day between 10.7 °C and 17.4 °C, recording a value at the time of data collection of 15 °C outside, and 16.7°C, with a relative humidity value between 38-40%. On the other hand, for the data recorded on the second day, January 15, the maximum and minimum temperature values reached values between 16.6 °C and 8.7 °C, registering a value of 13°C outside and 15.9 °C at the time of data collection, with a relative humidity value between 52%. During this second day, the rooms under deck 1 were analyzed, as well as the building annexed to the room under deck 2. The test consisted of analyzing the critical points detected during the visual inspection phases, in order to corroborate the results experimentally. In relation to the surface, a granular material with emissivity value 0.95 was considered based on the library of materials provided by the manufacturer, homogeneous for all the surfaces analyzed. Other published examples related to the emissivity of this type of materials can be found in (Barreira et al, 2021).

### 3. RESULTS AND DISCUSSIONS

In relation to the analysis of the water flow during the watertightness test, the results show that in the case of roof 1, the upper zone channels the water perimetrically towards the gutter through the established slopes. In the case of roof 1, in the lower zone, it was possible to verify that the slopes converge in the drainage area. The absence of overflows prevents the evacuation of water in the event of saturation of the drain due to the accumulation of solid elements at its entrance. This fact makes it easier for the level of stagnant water to reach the side wall of the Communion chapel, favoring the entry of water at the intersection of the vertical wall-skirt.

Regarding the results of the thermographic analysis of roof 1, Figure 3 shows the images for both the upper and lower areas of the roof. Figure 3 (a) shows an overview of the upper part of the roof. In this image, all the possible pathological manifestations previously mentioned can be identified. In the first place, it can be seen how after the watertightness test and the pouring of the water on part of the vertical façade enclosures and 10 h after the test, part of the humidity is preserved due to the high absorption capacity of the stone in the facing. In this image, it can also be seen how the area of the parapet, the water has accumulated more than in the area located just in the area of the gutter. A detail of this area can be seen in Figure 3c, where it can be observed not only the entry and accumulation of water in the lower area, but also the water filtered through the joints between the masonry pieces. On the other hand, it should also be noted the abrupt change in thermal characteristics at the joint between the parapet and the wall corresponding to the rigid protection of the upper skirt, Figure 3a-3c. The joint between the two materials is clearly observed and it can be seen how part of the water poured from the end of the skirt has dripped down the facing, being stored in the area of the joint, due to the absence of the correct realization of the detail of the end of the skirt. In relation to the gutter, however, no leakage problems have been detected. On the other hand, Figure 3b shows a detail of the gutter for the passage of the installations. In this image, it can be seen in green, the rear area of the gutter, where water has been stored, due to the lack of watertightness of the joint and the absence of a protection device to prevent water from dripping

down the face and leaking behind the gutter. On the other hand, Figure 3d shows a detail of the lack of watertightness of the right end of the parapet, in the area of connection of the end of the skirt, the parapet and the buttress, marking the area that is currently very deteriorated, being an obvious sign of lack of waterproofing. Also in relation to waterproofing problems, it can be seen in Figure 3e, the absence of the waterproofing in the contact area of the lower skirt with the parapet, as well as the presence of vegetation in the rightmost area of the photo, where the temperature is higher. In addition, the current state of waterproofing of the damaged area of the sill can be evaluated by means of this image. The results shown by thermography did not show the presence of watertightness problems. Finally, Figures 3g-3h show the dammed area during the test, where the process of capillary rise through the facing can be clearly observed, clearly exceeding the 5 cm of waterproofing strip currently in place at the junction of the skirt with the vertical facing, in the areas where it has been placed, since there is an absence of this construction detail in various parts of the lower skirt.

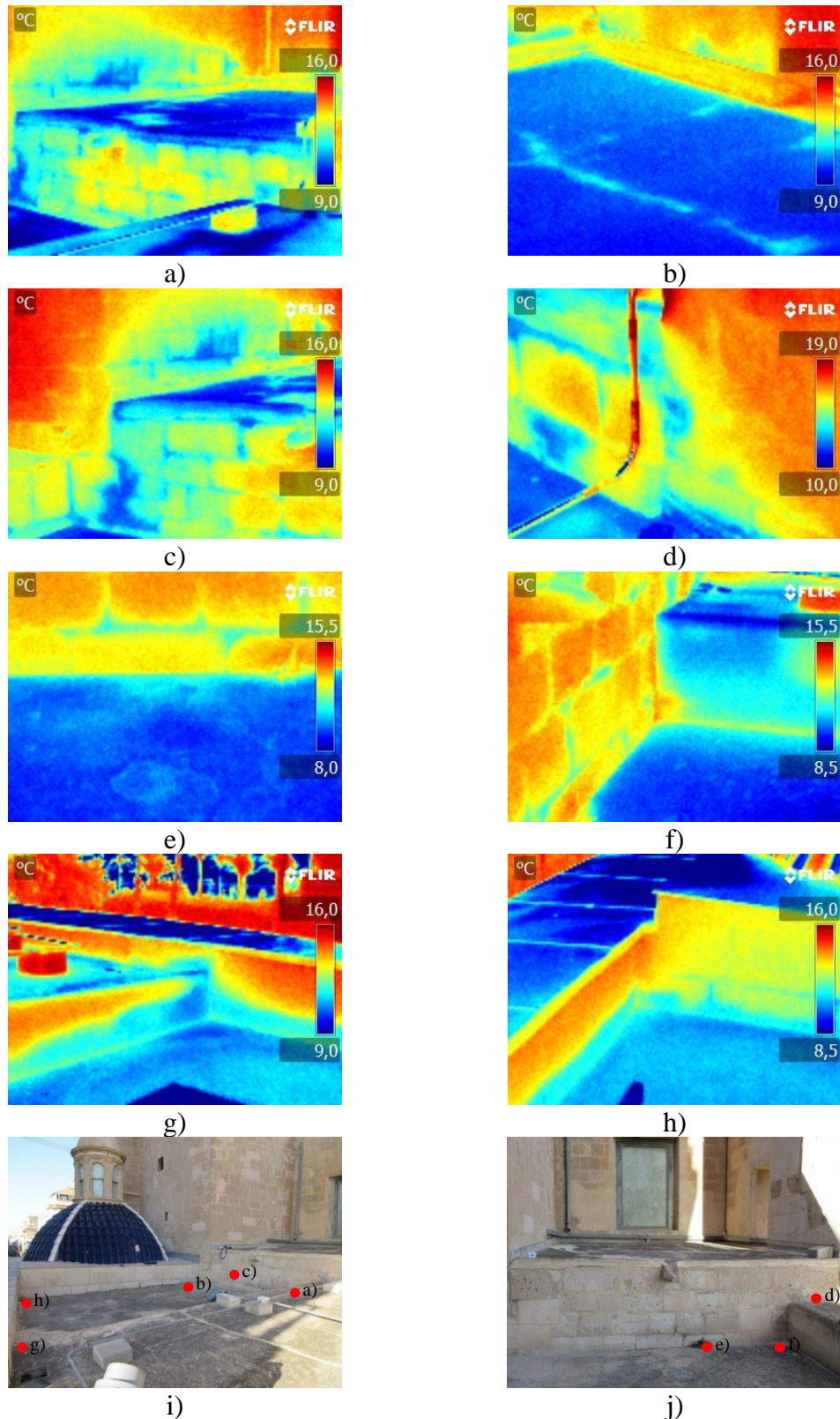


Figure 3. Thermography of roof 1: a) General view of the upper area, b) Detail of the installations gutter, c) Moisture in vertical facing and corner of parapet, filtration through masonry joints, d) Lack of watertightness in parapet and buttress, e) Lower skirt and vertical facing, f) Lateral connection of parapet skirt, g) and h) Capillarity, i) and j) location of the thermographs. The red dots indicate the location of the thermography in the associated image.

In relation to the results of the analysis of roof 2, Figure 4a and 4b show the detail of the absence of the perimeter joint, showing the difference in temperatures in the areas where the mortar is totally deteriorated, and the joint is without mortar between the end of the skirt and the facing. It is important not to confuse this with the red line associated with the passage of an installation pipe, since the area analyzed is the one associated with the end of the connection with the vertical face of the facade. These images show the lack of thermal insulation in the sections of the vertical facing, as well as areas with a colder tone, due to the water spilled during the load test. Figures 4c and 4d show a detail of this area without thermal camera application. On the other hand, Figure 4e shows the side skirt end zone. In this image it can be seen how the lack of thermal insulation in the vertical facing sections, as well as areas of colder tone, due to the water poured during the load test. This area is shown in a more greenish tone in the middle area of the photo. Also noteworthy is the contrast at the skirt end joint, clearly showing the position of the horizontal joint between the upper material and the support material. This joint, represented as a yellow line with cyan tones, presents an important state of deterioration, as could be observed during the visual analysis of the roof, Figure 4g. Finally, Figure 4f shows a detail of the perimeter end of the skirt, in the area near the access door to the roof. Figure 4 also includes digital camera images of the areas analyzed by thermal imaging. The comparison of these images allows observing the benefits of the use of thermography in the detection of pathologies, being this a support technique to the visual inspection.

On the other hand, Figures 5, 6 and 7 show the details of the temperature distribution inside the three interior rooms analyzed. It should be noted that due to the low levels of thermal differences between the different structural elements that make up the enclosure, the sharpness of the images does not show such a differentiated behavior as in the case of the analysis of the roofs. In order to increase the thermal contrast, in some rooms the spotlights were kept on before the test was carried out, in order to ensure the position of the edges of the room, once the thermal photos were taken, since these were taken with the light off.

Analyzing the thermal behavior of the room under the lower area of roof 1, Figure 5, referred to throughout the study as the room adjacent to the Communion Chapel, it can be seen in Figure 5a, corresponding to the corner of connection between the exterior facade and the main arch that gives access to the Communion Chapel and, arranged in the area near the presence of the drain in the roof at the top, that the thermal difference between the part corresponding to the facade and the roof of the vault is clearly defined. However, with the climatic conditions recorded during the test, the presence of specific thermal irregularities in the potentially damaged areas associated with the connection between the facade and the toral arch of the groin vault analyzed were not detected. Also, part of the exterior window is observed, which serves as a reference in order to be able to frame the photo. Figure 5b shows a detail of the window area. In this image, the cold spot effect is clearly visible due to the higher thermal transparency of the glass compared to the high thicknesses of the facade. In addition, the lack of thermal insulation in the connection areas between the facade and the roof can be observed, clearly marking the junction edge between the two, and showing a temperature gradient from the beginning to the central area of the vault. In Figure 5c, the thermography of the other corner of the exterior facade is shown, similar to that described in Figure 5a. As can be seen, in this image there are no relevant signs of pathology, being detected only the thermal gap between the vertical faces and the roof of the vault. Finally, Figure 5d shows a general image of the roof. This image shows the presence of a part of the roof slightly colder than the other, mainly due to the effect of the accumulation of water during the test.

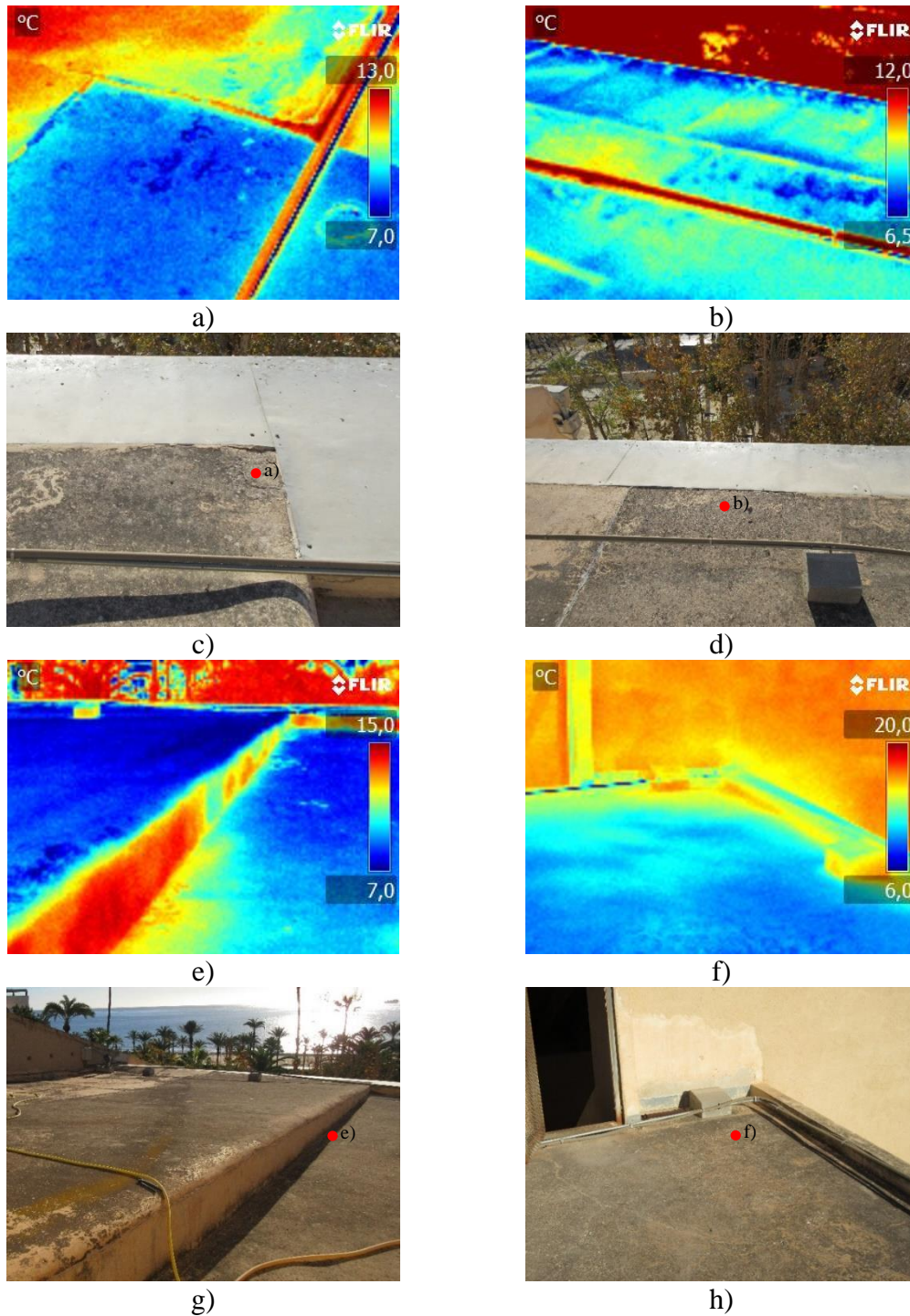


Figure 4. Thermography roof 2: a) Deterioration of perimeter joint, b) Detail of failure in perimeter joint in contact of the skirt with the facade, c) and d) Image a) and b) with digital camera, e) Detail of the lateral end of the skirt and connection with the roof, f) Perimeter zone of the skirt in the access area to the roof; g) and h) Image e) and f) with digital camera. The red dots indicate the location of the thermography in the associated image.

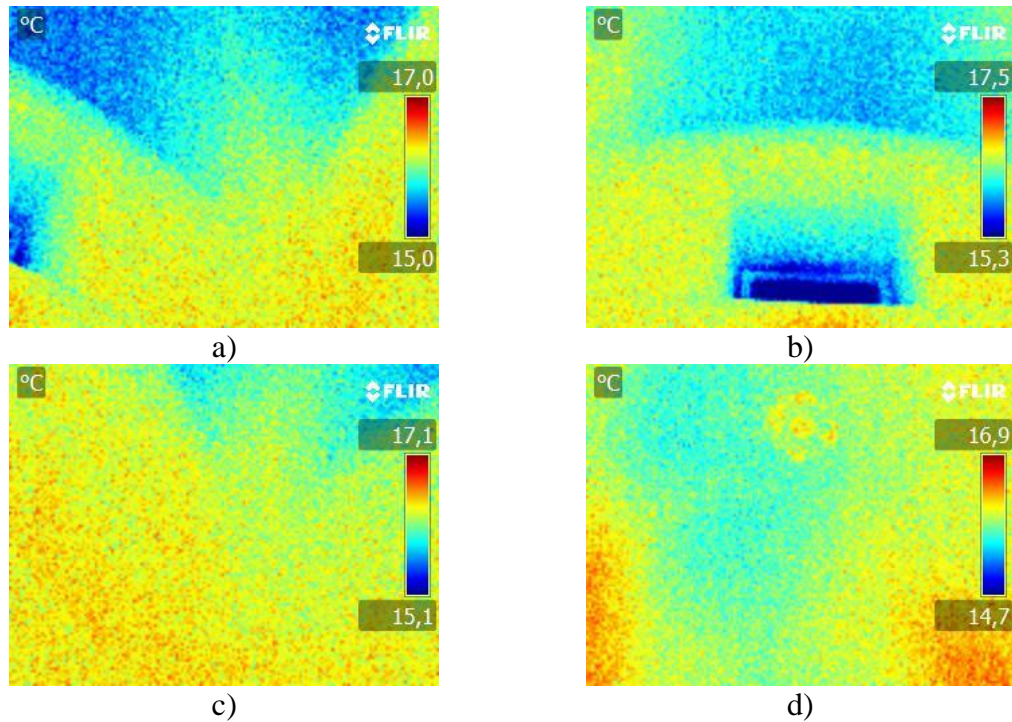


Figure 5. Thermography of rooms under roof 1, adjacent to the Communion Chapel: a) Connection of the main arch with the exterior facade, in the area of access to the Communion Chapel, b) Connection of the facade with the roof in the window area, c) Second corner of the facade wall, equivalent to image (a), d) General view of the roof from below.

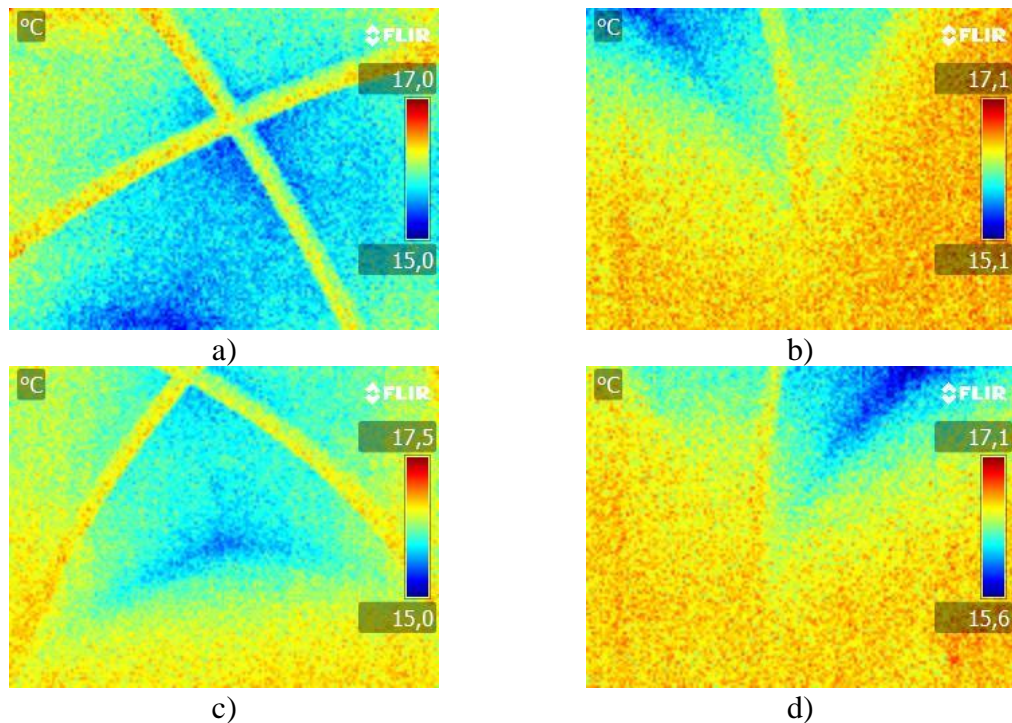


Figure 5. Thermography of rooms under roof 1, adjacent to the side building: a) General view of roof, b) Connection between facade and side corner, c) Connection between facade and roof, d) Connection between facade and opposite side corner.

In relation to the analysis by thermography carried out for the room located in the side nave, adjacent to the central nave of the basilica, Figure 6 shows the distribution of temperatures in the different critical points analyzed in the previous sections. First, Figure 6a shows a lower view of the groin vault roof. It can be observed the difference in temperatures between the perpendicular arches and the rest of the plementery that makes up the vault roof. On the other hand, Figure 6b and 6d show the detailed thermography of the connection corners between the perpendicular arches and the facade walls. A pattern of behavior similar to those described for the previous room is observed, with the difference of the higher temperature of the start of the arches. It should be noted that the analysis of these points was carried out without the presence of nearby light sources before or during the test, so the thermal distribution is due to the hygrothermal equilibrium between the exterior and the interior of the building. Finally, Figure 5c shows the same problem of lack of insulation as in the previous room, due to the connection joint between the vertical facing and the roof.

Finally, in relation to the thermography analysis carried out for the room under deck 2, Figure 7 shows the distribution of temperatures in the different critical points analyzed in the previous sections. In general, the thermal behavior is very similar to those detected in the previous rooms, except that in this case a high thermal difference between the points of the interior facade and the roof has not been observed. That is, Figures 7a, 7b, 7c and 7d show the detail of the contact between the facade and the roof, showing the thermal leaks in the upper part of the window area, as well as in the window itself. Figure 7e shows a thermography of the part of the roof corresponding to the anchorage of the chandelier, where a uniform distribution of temperatures is observed without the presence of detected damage. In Figures 7f and 7g, the thermographies associated to Figures 7c and 7d are observed, but in this case, in the facade opposite to the exterior one. In this case, the thermal variations can be observed in the areas affected by the heating of the light sources. This is due to the presence of cold spots in the contact zones between the side wall and the facade. These cold spots, especially those detected in Figure 7g, are related to the detected moisture stains. In these images, the coldest circular hole is shown as a reference to locate the position of the photos. It is important to point out that such humidity stains, besides being related to the presence of a cold zone, are also related to the presence of a water accumulation zone in the upper part of deck 2, close to the dome. In this area the water collected in the dome is discharged, and the lack of lateral sealing at the end of the skirt, together with the low level of ventilation in the room shown, cause the increase in humidity, and thus the appearance of such efflorescence.

Finally, it should be noted the presence of a leak detected in the annex building with access to room 2. This leak is on the roof of the upper floor. It has not been possible to detect whether the presence of moisture is due to an error in the tile roof, or in the roof 2 itself. However, due to its geometric position, it is very close to the position of the roof drain, which could be a sign of a lack of watertightness of the roof.

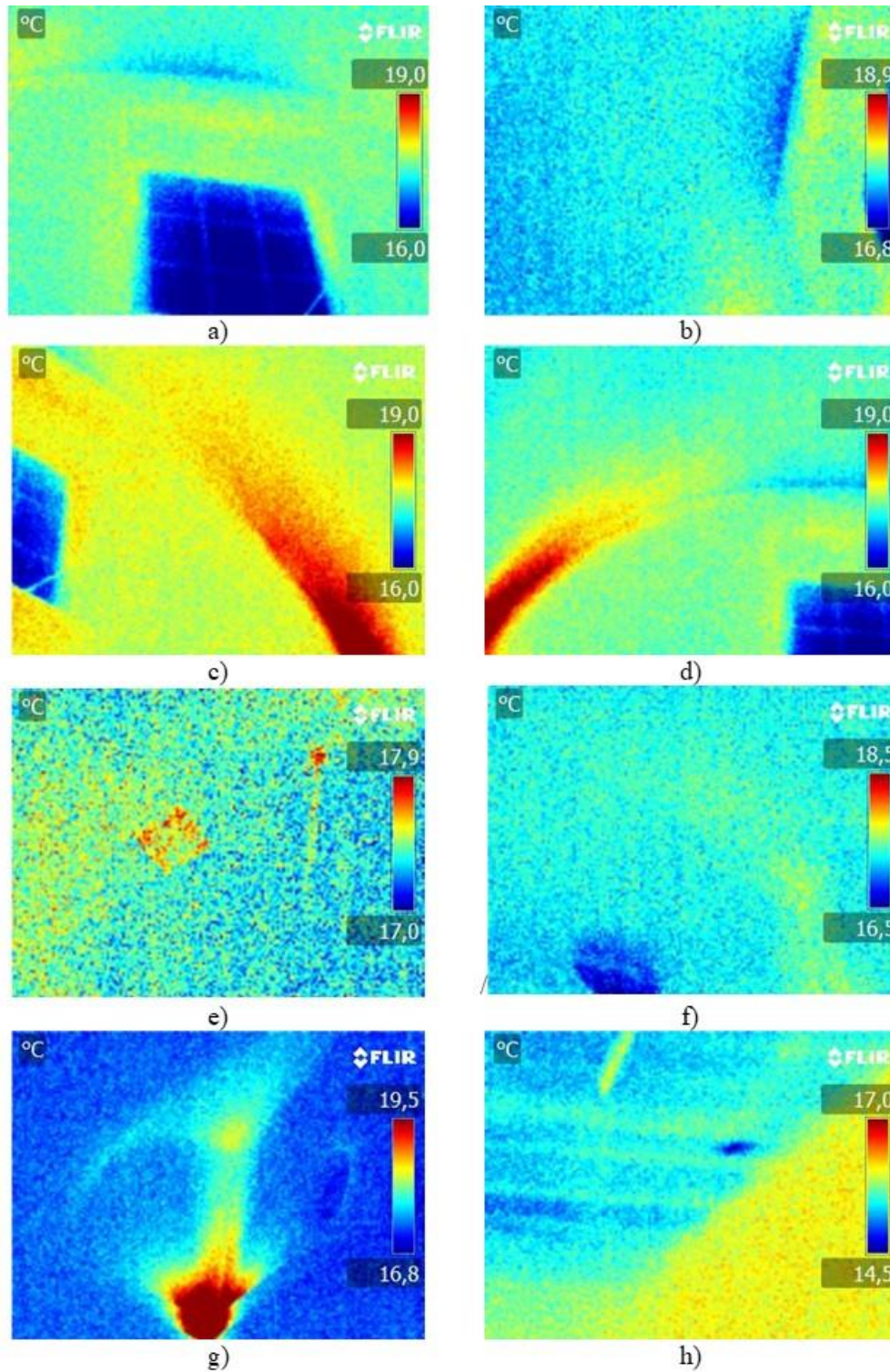


Figure 7. Thermography of room under roof 2: a) window and slab area, b) lower view of roof, c) connection view of slab side wall, d) connection view of slab side wall, e) central area of roof, f) view of rear dividing wall, g) connection view of side wall and rear wall, h) leak in outbuilding area.

## 4. CONCLUSIONS

After carrying out the technical assessment study of the state of watertightness and the analysis of humidities of the roofs analyzed in the basilica of Santa Maria, it can be concluded that the current state of the roof does not meet the minimum technical conditions based on the current state of the construction details according to the provisions of the regulations (NBE QB-90). Likewise, the state of humidity and efflorescence present in the interior areas is due to a problem of hygroscopic condensation, because the humidity increases due to the proximity to the maritime area, as well as the lack of ventilation of the interior rooms studied. In addition, this pathology is intensified by the possible filtration problems caused during the months of October and November, due to the higher level of rainfall. This water accumulates in the interior of the construction elements and eliminates excess humidity by vapor transmission as the thermal conditions of the building change. In addition, the presence of sea salts in nearby buildings and the high absorption capacity of the materials studied, show a behavior prone to the dragging of salts in solution during the rainy season, which favors the appearance of efflorescence, which increases the risk of condensation moistures. On the other hand, in relation to the use of thermographic analysis techniques, the images have made it possible to detail existing pathologies with greater precision, especially those due to thermal leaks and areas of moisture accumulation, which are imperceptible during visual exploration. This fact highlights the feasibility of using thermography to identify pathologies in masonry buildings that could be hidden by coatings or geometric conditions that prevent their detection with the naked eye. In addition, by using this technique it is possible to more accurately delimit the repair surfaces from the point of view of a future intervention compared to a direct visual analysis without thermography as commented by Barbosa (Barbosa et al, 2021).

## 5. ACKNOWLEDGEMENTS

The authors wish to thank the Bishopric of Orihuela-Alicante for their willingness to carry out this study on a catalogued property.

## 6. REFERENCES

- Barbosa, M.T.G., Rosse, V. J., Laurindo, N. G. (2021), “*Thermography evaluation strategy proposal due moisture damage on building facades*”, Journal of Building Engineering, 43, art. no. 102555, DOI: <https://doi.org/10.1016/j.jobbe.2021.102555>
- Barreira, E., Almeida, R.M.S.F., Simões, M.L., Rebelo, D. (2020), “*Quantitative infrared thermography to evaluate the humidification of lightweight concrete*”, Sensors (Switzerland), 20 (6), art. no. 1664, DOI: <https://doi.org/10.3390/s20061664>
- Barreira, E., Almeida, R.M.S.F., Simões, M.L. (2021), “*Emissivity of building materials for infrared measurements*”, Sensors, 21 (6), art. no. 1961, pp. 1-13. DOI: <https://doi.org/10.3390/s21061961>
- Bevià García, M., Azuar Ruiz, R. (2005), “*Santa María descubierta: Arqueología, arquitectura-cerámica: Excavaciones en la Iglesia de Santa María de Alicante (1997-1998)*”. Alicante. Fundación MARQ. ISBN: 84-609-7478-2
- Brotóns, V., Tomás, R., Ivorra, S., Alarcón, J.C. (2013), “*Temperature influence on the physical and mechanical properties of a porous rock: San Julian's calcarenite*. Engineering Geology”, 167, pp. 117-127. DOI: <https://doi.org/10.1016/j.enggeo.2013.10.012>

- Giovannacci, D., Brissaud, D., Mertz, J.-D., Mouhoubi, K., Bodnar, J.-L. (2017), “*Nonintrusive tools to detect salts contamination in masonry: Case study of Fontaine-Chaalis church*”, Proceedings of SPIE - The International Society for Optical Engineering, 10331, art. no. 1033103. DOI: <https://doi.org/10.1117/12.2269727>
- Grossi, C. M. Esbert, R. M. (1994), “*Las sales solubles en el deterioro de rocas monumentales. Revisión bibliográfica*”. Materiales de Construcción, Vol. 44, nº 235. DOI: <https://doi.org/10.3989/mc.1994.v44.i235.579>
- Louis, M., García del Cura, M. A., Spairani, Y., de Blas. D. (2001), “*The Civil Palaces in Gravina Street, Alicante: building stones and salt weathering*. Materiales de Construcción”, Vol. 51, nº262. DOI: <https://doi.org/10.3989/mc.2001.v51.i262.369>
- Lucchi, E. (2018), “*Applications of the infrared thermography in the energy audit of buildings: A review*”, Renewable and Sustainable Energy Reviews, 82, pp. 3077-3090. DOI: <https://doi.org/10.1016/j.rser.2017.10.031>
- Paricio Ansuateguie, I. “*La construcción de la Arquitectura. Institut de Tecnologia de la Construcció de Catalunya*”, 1985, T.2, p. 26. ISBN: 978-84-7853-375-6
- Norma Básica de la Edificación. Cubiertas con materiales bituminosos: “*NBE QB-90*”. Gobierno de España.
- Ruiz Valero, L., Flores Sasso, V., Prieto Vicioso, E. (2019), “*In situ assessment of superficial moisture condition in façades of historic building using non-destructive techniques*”, Case Studies in Construction Materials, 10, art. no. e00228, DOI: <https://doi.org/10.1016/j.cscm.2019.e00228>
- Silva, G. P., Batista, P. I. B., Povóas, Y. V. (2019), “*Uso de termografía infrarroja para estudiar el desempeño térmico de paredes: una revisión bibliográfica*”, Revista ALCONPAT, 9(2), pp. 117 – 129, DOI: <http://dx.doi.org/10.21041/ra.v9i2.341>
- Takeda, T. Mazer, W. (2018), “*Potencial da análise termográfica para avaliar manifestações patológicas em sistemas de revestimentos de fachadas*”, Revista ALCONPAT, 8 (1), pp. 38 – 50, DOI: <http://dx.doi.org/10.21041/ra.v8i1.181>
- Valluzzi, M.R., Lorenzoni, F., Deiana, R., Taffarel, S., Modena, C. (2019), “*Non-destructive investigations for structural qualification of the Sarno Baths, Pompeii*”, Journal of Cultural Heritage, 40, pp. 280-287. DOI: <https://doi.org/10.1016/j.culher.2019.04.015>
- Vijay, P.V., Tulasi Gadde, K., Gangarao, H.V.S. (2019), “*Structural Evaluation and Rehabilitation of Century-Old Masonry and Timber Buildings*”, Journal of Architectural Engineering, 25 (2), art. no. 05019001, DOI: [https://doi.org/10.1061/\(ASCE\)AE.1943-5568.0000350](https://doi.org/10.1061/(ASCE)AE.1943-5568.0000350)
- Garrido, I., Solla, M., Lagüela, S., Fernández, N. (2020), “*Irt and gpr techniques for moisture detection and characterisation in buildings*”, Sensors (Switzerland), 20 (22), art. no. 6421, pp. 1-38. DOI: <https://doi.org/10.3390/s20226421>
- Martínez-Garrido, M.I., Fort, R., Gómez-Heras, M., Valles-Iriso, J., Varas-Muriel, M.J. (2018), “*A comprehensive study for moisture control in cultural heritage using non-destructive techniques*”, Journal of Applied Geophysics, 155, pp. 36-52. DOI: <https://doi.org/10.1016/j.jappgeo.2018.03.008>
- Zhang, F., Zhang, X., Li, Y., Tao, Z., Liu, W., He, M. (2018), “*Quantitative description theory of water migration in rock sites based on infrared radiation temperature*”, Engineering Geology, 241, pp. 64-75. DOI: <https://doi.org/10.1016/j.enggeo.2018.05.006>

Thomas, c., Lombillo, I., Setién, J., Polanco, J. A., Villegas, L. (2008), “*Absorción por capilaridad y consolidación de materiales pétreos del patrimonio histórico construido impermeabilizados y reforzados con productos hidrofugantes y consolidantes comerciales*”. Tecnología de la rehabilitación y la gestión del patrimonio construido (REHABEND). ISBN: 978-84-692-5650-3.

UNE EN 13187 (1998). “*Prestaciones térmicas de edificios. Detección cualitativa de irregularidades en cerramientos de edificios. Método de infrarrojos*”. Asociación Española de Normalización.